

A MATHEMATICAL MODEL OF A DIPHTHERIA OUTBREAK IN ROHINGYA SETTLEMENT IN BANGLADESH

A. AKTER AKHI[✉], F. TASNIM^{ORCID}, S. AKTER^{ORCID}, AND MD. KAMRUJJAMAN^{ORCID}

Article type: Research Article

(Received: 06 May 2022, Received in revised form: 07 January 2023)

(Accepted: 24 February 2023, Published Online: 24 February 2023)

ABSTRACT. In this paper, we study the dynamics of the diphtheria outbreak among the immunocompromised group of people, the Rohingya ethnic group. Approximately 800,000 Rohingya refugees are living in the Balukhali refugee camp in Cox's Bazar. The camp is densely populated with the scarcity of proper food, healthcare, and sanitation. Subsequently, in November 2017 a diphtheria epidemic occurred in this camp. To keep up with the pace of the disease spread, medical demands, and disaster planning, we set out to predict diphtheria outbreaks among Bangladeshi Rohingya immigrants. We adopted a modified Susceptible-Latent-Infectious-Recovered (SLIR) transmission model to forecast the possible implications of the diphtheria outbreak in the Rohingya camps of Bangladesh. We discussed two distinct situations: the daily confirmed cases and cumulative data with unique consequences of diphtheria. Data for statistical and numerical simulations were obtained from [1]. We used the fourth-order Runge-Kutta method to obtain numerical simulations for varying parameters of the model which would demonstrate conclusive estimates. Daily and cumulative data predictions were explored for alternative values of the parameters, i.e., disease transmission rate (β) and recovery rate (γ). Additionally, the average basic reproduction number for the parameters β and γ was calculated and displayed graphically. Our analysis demonstrated that the diphtheria outbreak would be under control if the maintenance could perform properly. The results of this research can be utilized by the Bangladeshi government and other humanitarian organizations to forecast disease outbreaks. Furthermore, it might help them to make detailed and practical planning to avoid the worst scenario.

Keywords: SLIR model, Diphtheria, Stability analysis, Model validation, Numerical analysis.

2020 MSC: Primary 37N25, 49J15, 92D30.

✉ kamrujjaman@du.ac.bd, ORCID: 0000-0002-4892-745X

DOI: 10.22103/jmmr.2023.19459.1256

Publisher: Shahid Bahonar University of Kerman

How to cite: A. Akter Akhi, F. Tasnim, S. Akter, and M. Kamrujjaman, *A mathematical model of a diphtheria outbreak in Rohingya settlement in Bangladesh*, J. Mahani Math. Res. 2023; 12(2): 547-563.



© the Authors

1. Introduction

SIR model is a fundamental infectious disease transmission model, introduced in the early 20th Century [2, 3]. Infectious diseases caused by microorganisms such as bacteria, viruses, and parasites, spread through various forms of physical contact, including sneezing, coughing, or breathing; feces, blood, and other bio-fluids are also common sources of transmission [3, 4]. Despite the significant growth of modern medical technologies, we are not immunized to these life-threatening microscopic organisms. The Covid-19 pandemic opened our eyes and showed the world how vulnerable we are [5, 6]. Some well-known epidemics from primitive times are the Plague of Athens (430-438 B.C.), Circa (3000 B.C.), Plague of Justinian (541-542), Black Death (14th Century), and Spanish Flu (20th Century). The realistic nature of epidemiology has attracted numerous researchers in this field of mathematical biology. Real-time modeling can make it possible to find vital information about the potentiality of an epidemic [7], like collecting required resources and underlying mechanisms of disease transmission to make decisions for the future [8, 9].

Diphtheria is a contagious respiratory disease spread by a strain of bacteria known as *Cyanobacteria*, generally through air droplets, and its transmission can be prevented by employing widespread vaccination measures. Tracing and identifying infected individuals with Diphtheria symptoms may help reduce transmission. Some common symptoms are fever, fatigue, scratchy throat, and swollen glands. Fatal damage might occur in vital organs like the kidney, and heart leading to breathing issues, cardiac arrest, and even death [1]. Vaccination measures have led to the eradication of diphtheria in developed nations; hence there is a limitation of epidemiological data [1, 10–12]. Despite these immunization measures, Thailand has reported multiple diphtheria flare-ups in the past few decades, including the 2012 outbreak [13].

Refugee camps often suffer from outbreaks of infectious diseases such as cholera, hepatitis, and diphtheria as a consequence of inadequate hygiene and poor living standards. Following the collapse of the former soviet union in 1990, an outbreak of diphtheria occurred, and the epidemic curve peaked during the mid-nineties with almost a million reported cases [14]. Moreover, in some conflict settings in Yemen and Venezuela, there are reported diphtheria outbreaks [1, 15].

A massive diphtheria outbreak occurred in the overcrowded refugee camp of Southern Bangladesh in November of 2017. By the end of 2019, the number of cases mounted up to a total of 7064 with just 4% confirmed through diagnosis [16]. In the last couple of decades, the Rohingya people have been victims of a forced exodus and have been living as refugees in Bangladesh. In August 2017, about 625000 Rohingyas fled Myanmar and moved into the largest refugee settlement in Bangladesh [8, 17]. Due to lifelong undernourishment and the absence of healthcare, the camp has often faced outbreaks of various contagious diseases like diarrhea, malaria, dengue, measles, and chikungunya [15, 18].

Moreover, the descent of the COVID-19 pandemic has not been kind to this distressed community [19]. The impact of SARS-CoV-2 infection in the Rohingya Refugee camp has been explored by [20]. The main objective of this article is,

- To investigate the dynamics of the diphtheria outbreak in the Rohingya camp in Bangladesh using the Susceptible-Latent-Infectious-Recovered (SLIR) epidemic model.

The main novelty and findings of this study are as follows:

- This study analyzes a modified Susceptible-Latent-Infectious-Recovered (SLIR) ODE model along with the non-negativity and boundedness of solutions.
- We have formulated the disease-free equilibrium points and basic reproduction numbers corresponding to the required system of first-order ordinary differential equations (ODEs) following various parameters.
- Numerical illustrations have been performed to observe the effects of disease transmission rate and recovery rate on the dynamics of the disease outbreak.
- The strategy for controlling the diphtheria outbreak is suggested.

This work investigates the diphtheria epidemiological data set from the Rohingya refugee camp. The article's structure is as follows: Section 2 details the SLIR mathematical model. A similar compartmental model on the COVID-19 pandemic considered a non-linear incidence rate [21]. Non-negativity and boundedness of solutions are presented in sub-Section 2.1. Section 3 covers the suggested model's equilibrium point. A brief calculation to determine the basic reproduction number has been depicted in Section 4. Results and discussions are found in Section 5. We have also conveyed numerical methods and parameter estimation for the system in sub-Section 5.1. Furthermore, numerical illustrations with suitable pictorial representation are outlined in sub-Section 5.2. Finally, Section 6 shows the conclusion of the results.

2. Mathematical Model

In this paper, we propose the following SLIR (Susceptible-Latent-Infectious-Recovered) epidemic model to explore the dynamics of diphtheria spread in the Rohingya settlement [24, 25],

$$(1) \quad \begin{cases} \frac{dS}{dt} = \Lambda - \beta S(t)I(t) - \mu S(t), \\ \frac{dL}{dt} = l\beta S(t)I(t) - (\mu + \delta)L(t), \\ \frac{dI}{dt} = (1-l)\beta S(t)I(t) + \delta L(t) - (\mu + \gamma + \alpha)I(t), \\ \frac{dR}{dt} = \gamma I(t) - \mu R(t), \end{cases}$$

for $t \in (0, \infty)$ the non-negative initial conditions are,

$$(2) \quad S(0) = S_0, \quad L(0) = L_0, \quad I(0) = I_0, \text{ and } R(0) = R_0.$$

The diagram depicting the transition of this compartmental model (1) is shown in Figure 1.

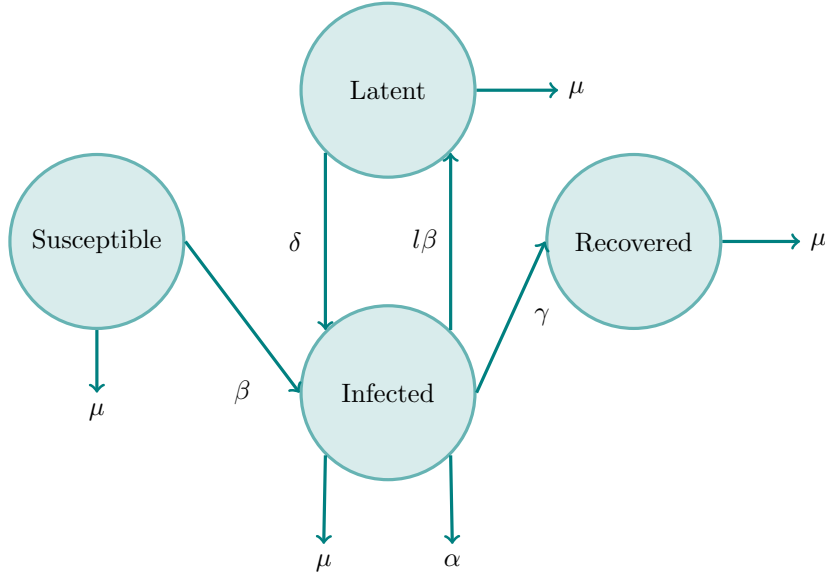


FIGURE 1. Schematic diagram of transmission dynamics of SLIR model.

It should be noted that,

$$N(t) \equiv S(t) + L(t) + I(t) + R(t),$$

$$\frac{dN}{dt} \equiv \frac{dS}{dt} + \frac{dL}{dt} + \frac{dI}{dt} + \frac{dR}{dt}.$$

Here, $N(t)$ is the total number of individuals which is subdivided into four compartments S, L, I , and R which represent the number of populations in the susceptible, latent, infected, and recovered class, respectively. Hence, for the system (1), $\frac{dN}{dt} = \Lambda - \mu N(t) - \alpha I(t)$. The parameter Λ is the recruitment rate of the susceptible class, it is defined as $\frac{S_0}{\mu}$, where μ is the natural mortality rate. Moreover, α signifies the disease-induced death rate. The infection transmission rate is denoted by β . δ stands for the detection rate of the latent population, and l restricts the infection for the L class. Following this, the detection rate δ regulates the transition from the L class to the I class.

2.1. Non-negativity and boundedness of solutions. Let us define

$$K = \frac{\Lambda}{\mu}.$$

Now it is possible to define the model (1) in compact form with some initial set of data,

$$(3) \quad \mathbf{U}' = F(\mathbf{U}, t), \quad U(0) = U_o.$$

where $\mathbf{U} = (U_1, U_2, U_3, U_4) = (S, L, I, R)$. Now the system (3) maintains existence and uniqueness theory for differential equations, considering the function F is C^1 and locally Lipschitz in \mathbf{U} . Now, in order to prove positivity and boundedness for the interval $(0, T)$, where T and $U(t)$ are finite, we show the set Φ is invariant under the system flow,

$$\Phi = \{\mathbf{U} \in \mathbb{R}^4 : U_i \geq 0, \sum_{i=1}^4 U_i < K\}.$$

and the set Φ is positively invariant under the flow $U(t)$ for $t \in (0, T)$ and therefore $T = \infty$, implying that the solution exists globally in time.

Theorem 2.1. *The closed region $\Phi = \{\mathbf{U} \in \mathbb{R}^4 : U_i \geq 0, \sum_{i=1}^4 U_i < K\}$ is positive and bounded for the system (1) [20].*

Proof. The boundary component Π for $i = \overline{1, 5}$, are denoted by,

$$\Pi_i = \{\mathbf{U} \in \Phi : U_i = 0, \quad i = \overline{1, 4}\},$$

$$\Pi_5 = \{\mathbf{U} \in \Phi : \sum_{i=1}^5 U_i = K\},$$

where, $\partial\Phi = \cup_{i=1}^5 \Pi_i$. Furthermore, the inward normal \mathbf{n}_i , defined for the boundary segments Π_i , $i = \overline{1, 4}$, $\mathbf{n}_i = \eta_i = (0, 0, 1, 0, 0)$ where the i -component is nonzero, and $\mathbf{n}_5 = (-1, -1, -1, -1, -1)$. Here, \mathbf{n} is the positive linear combination of the inward normal of the boundary segments. Our proof will be done if, $\mathbf{n} \cdot \mathbf{U}(t) \geq 0$. Now, for $i = \overline{1, 4}$ and $\sum_{i=1}^5 U_i = K$,

$$\eta_1 \cdot \mathbf{U}' = \Lambda \geq 0, \quad \text{for } \mathbf{U} \in \Pi_1,$$

$$\eta_2 \cdot \mathbf{U}' = l\beta U_1 U_3 \geq 0, \quad \text{for } \mathbf{U} \in \Pi_2,$$

$$\eta_3 \cdot \mathbf{U}' = \delta U_2 \geq 0, \quad \text{for } \mathbf{U} \in \Pi_3,$$

$$\eta_4 \cdot \mathbf{U}' = \gamma U_3 \geq 0, \quad \text{for } \mathbf{U} \in \Pi_4.$$

Considering, $\sum_{i=1}^5 U_i = K$, we get,

$$\frac{dN}{dt} = \Lambda - \mu N(t) - \alpha I(t).$$

Let $N = K$ for a constant K . On Π_5 , we have,

$$\mathbf{n}_5 \cdot \mathbf{U}' = -\Lambda + \mu K + \alpha U_3 \geq 0.$$

Thus, our proof is complete, since Φ is positively invariant. It should be noted that for chosen initial conditions $U_0 \in \Phi$, the solution $U_t \in \Phi$ exists. \square

3. Equilibrium Point

To determine the equilibrium points of the compartment model (1), we resolve the system by setting each derivative equal to zero. It is assumed, at equilibrium steady states, $(S, L, I, R) \equiv (S^*, L^*, I^*, R^*)$. We have,

$$(4) \quad \begin{cases} \Lambda - \beta S^* I^* - \mu S^* = 0, \\ l\beta S^* I^* - (\mu + \delta)L^* = 0, \\ (1-l)\beta S^* I^* + \delta L^* - (\mu + \gamma + \alpha)I^* = 0, \\ \gamma I^* - \mu R^* = 0. \end{cases}$$

3.1. Disease-free Equilibrium Point (DFE). For finding DFE point, we substitute the variables by the following manner, $(S^*, L^*, I^*, R^*) \equiv (S^0, L^0, I^0, R^0)$. Thus, we move,

$$(5) \quad \begin{cases} \Lambda - \beta S^0 I^0 - \mu S^0 = 0, \\ l\beta S^0 I^0 - (\mu + \delta)L^0 = 0, \\ (1-l)\beta S^0 I^0 + \delta L^0 - (\mu + \gamma + \alpha)I^0 = 0, \\ \gamma I^0 - \mu R^0 = 0. \end{cases}$$

After finishing easy calculation, we finally get our desired DFE point as $(S^0, L^0, I^0, R^0) = (\frac{\Lambda}{\mu}, 0, 0, 0)$.

4. Basic Reproduction of the Model

In epidemiology, the basic reproduction number is sometimes called the basic reproductive ratio or incorrectly basic reproductive rate. It is denoted by R_0 . By observing the work of Alfred Lotka, Ronald Ross, and others, it is possible to understand the root concept of the basic reproduction ratio. At first, George MacDonald applied this basic reproduction number in modern epidemiology in 1952. The basic reproductive number helps to predict the disease outbreak of a disease.

The basic reproduction number is a crucial threshold analysis of infectious disease modeling. It is useful to determine whether or not an infectious disease can accelerate through a population [26].

An epidemic will exist in the population only if an infected individual appears in it. The basic reproduction number or threshold parameter R_0 is particularly important when analyzing the transmission dynamics of any illness, because if,

- (1) $R_0 < 1$, there will be no epidemic or disease will die out.
- (2) $R_0 > 1$, the epidemic will occur or disease will persist.

4.1. Calculation of R_0 . There are several ways to calculate basic reproduction numbers. Among them, the next-generation approach is a flourishing technique that is easy to design. For the next-generation approach in the SLIR model, suppose,

$$\mathcal{F} = \begin{pmatrix} l\beta SI \\ (1-l)\beta SI \\ 0 \end{pmatrix} \quad \text{and} \quad \mathcal{V} = \begin{pmatrix} (\mu + \delta)L \\ (\mu + \gamma + \alpha)I - \delta L \\ \mu R - \gamma I \end{pmatrix},$$

where \mathcal{F} incorporates the rate of appearance of a new infection, and \mathcal{V} shows the remaining intermediate terms, like mortality rate, deaths, recovery, and others. Then, determine the matrices F and V ,

$$F = \begin{pmatrix} 0 & l\beta S & 0 \\ 0 & (1-l)\beta S & 0 \\ 0 & 0 & 0 \end{pmatrix} \quad \text{and} \quad V = \begin{pmatrix} \mu + \delta & 0 & 0 \\ -\delta & \mu + \gamma + \alpha & 0 \\ 0 & -\gamma & \mu \end{pmatrix}.$$

Therefore, the inverse matrix of V , and the next-generation matrix FV^{-1} becomes,

$$V^{-1} = \begin{pmatrix} \frac{1}{\delta + \mu} & 0 & 0 \\ \frac{\delta}{(\alpha + \gamma + \mu)(\delta + \mu)} & \frac{1}{\alpha + \gamma + \mu} & 0 \\ \frac{\gamma\delta}{\mu(\alpha + \gamma + \mu)(\delta + \mu)} & \frac{\gamma}{\mu(\alpha + \gamma + \mu)} & \frac{1}{\mu} \end{pmatrix},$$

$$FV^{-1} = \begin{pmatrix} \frac{l\beta S\delta}{(\alpha + \gamma + \mu)(\delta + \mu)} & \frac{l\beta S}{(\alpha + \gamma + \mu)} & 0 \\ \frac{(1-l)\beta S\delta}{(\alpha + \gamma + \mu)(\delta + \mu)} & \frac{(1-l)\beta S}{(\alpha + \gamma + \mu)} & 0 \\ 0 & 0 & 0 \end{pmatrix}.$$

Thus, spectral radius, $\sigma(FV^{-1}) = \frac{\Lambda(l\beta\delta - (-1+l)\beta(\delta + \mu))}{\mu(\alpha + \gamma + \mu)(\delta + \mu)} = \frac{\Lambda\beta(\delta + \mu - l\mu)}{\mu(\alpha + \gamma + \mu)(\delta + \mu)}$.

In the next generation approach, this spectral radius is the basic reproduction number R_0 . Hence,

$$(6) \quad R_0 = \frac{\Lambda\beta(\delta + \mu - l\mu)}{\mu(\alpha + \gamma + \mu)(\delta + \mu)}.$$

For DFE point, we set $I = 0$. On the other hand, for endemic equilibrium (EE) point $I \neq 0$.

To calculate the infective singularity or endemic equilibrium state of the system (1), we consider,

$$\frac{dS}{dt} = \frac{dL}{dt} = \frac{dI}{dt} = \frac{dR}{dt} = 0.$$

We obtain the endemic equilibrium point by solving the aforementioned system. After some simplification, we get the EE point,

$$\mathbf{E} = (S_1, L_1, I_1, R_1).$$

where

$$S_1 = \frac{(\delta + \mu)(\gamma + \delta + \mu)}{\beta(\delta + \mu - l\mu)}, \quad L_1 = \frac{l\Lambda}{\delta + \mu} - \frac{l\Lambda(\gamma + \delta + \mu)}{\beta(\delta + \mu - l\mu)},$$

$$I_1 = \frac{\mu}{\beta}(R_0 - 1), \quad R_1 = -\frac{\gamma}{\beta} + \frac{\gamma\Lambda(\delta + \mu - l\mu)}{\mu(\delta + \mu)(\gamma + \delta + \mu)}.$$

The formulations of the I_1 make it clear that the EE point will only exist when $R_0 > 1$. Furthermore, the Jacobian matrix of the model (1) at EE point (S_1, L_1, I_1, R_1) is calculated by,

$$\mathbb{J}(S_1, L_1, I_1, R_1) = \begin{pmatrix} -\mu - \frac{l\beta\Lambda}{\delta + \mu} + \frac{l\mu(\gamma + \delta + \mu)}{\delta + \mu - l\mu} & 0 & -\frac{(\delta + \mu)(\gamma + \delta + \mu)}{\delta + \mu - l\mu} & 0 \\ l^2 \left(\frac{\beta\Lambda}{\delta + \mu} - \frac{\mu(\gamma + \delta + \mu)}{\delta + \mu - l\mu} \right) & -\delta - \mu & \frac{l(\delta + \mu)(\gamma + \delta + \mu)}{\delta + \mu - l\mu} & 0 \\ (l-1)\beta \left(-\frac{l\Lambda}{\delta + \mu} + \frac{l\mu(\gamma + \delta + \mu)}{\delta + \mu - l\mu} \right) & \delta & -\frac{l\delta(\gamma + \delta + \mu)}{\delta + \mu - l\mu} & 0 \\ 0 & 0 & \gamma & -\mu \end{pmatrix}.$$

The determinant of this matrix is,

$$\text{Det}(\mathbb{J}) = -\frac{l\mu(\gamma + \delta + \mu)(\mu(\delta + \mu)(\gamma + \delta + \mu) - \beta\Lambda(\delta + \mu - l\mu))}{\delta + \mu - l\mu} < 0.$$

which satisfies the Li and Muldowney theorem of stability [22].

One of the roots of the characteristic equation $\text{Det}(\mathbb{J} - \lambda\mathbb{I}) = 0$ is $\lambda_1 = -\mu$, and the remaining three roots can be determined by using the following quadratic equation,

$$(7) \quad \lambda^3 + Q_1\lambda^2 + Q_2\lambda + Q_3 = 0.$$

where

$$Q_1 = -(P_1 + P_6 + P_7), Q_2 = P_1P_7 + P_1P_6 + P_6P_7 - P_2P_5 - P_4\delta, Q_3 = P_2P_5P_7 + P_1P_4\delta - P_1P_6P_7 - P_2P_3\delta,$$

$$\text{and } P_1 = -\mu - \frac{l\beta\Lambda}{\delta + \mu} + \frac{l\mu(\gamma + \delta + \mu)}{\delta + \mu - l\mu}, P_2 = -\frac{(\delta + \mu)(\gamma + \delta + \mu)}{\delta + \mu - l\mu}, P_3 = l^2 \left(\frac{\beta\Lambda}{\delta + \mu} - \frac{\mu(\gamma + \delta + \mu)}{\delta + \mu - l\mu} \right),$$

$$P_4 = \frac{l(\delta + \mu)(\gamma + \delta + \mu)}{\delta + \mu - l\mu}, P_5 = (l-1)\beta \left(-\frac{l\Lambda}{\delta + \mu} + \frac{l\mu(\gamma + \delta + \mu)}{\delta + \mu - l\mu} \right),$$

$$P_6 = -\frac{l\delta(\gamma + \delta + \mu)}{\delta + \mu - l\mu}, P_7 = -\delta - \mu.$$

All the roots of the characteristic equation $\text{Det}(\mathbb{J} - \lambda\mathbb{I}) = 0$ will have the negative real part for $R_0 > 1$ which satisfy the necessary condition of the Routh–Hurwitz criterion [23]. Thus, the EE point is locally asymptotically stable.

5. Results and Discussion

5.1. Numerical Method and Parameter Estimation. The concerned model (1) is a first-order ordinary differential equation (ODE) with initial conditions. To find the numerical solution of first order ODE, the most renowned numerical methods are the Euler method, Adams-Moulton method, backward differentiation method (BDF), linear multistep method, or Runge-Kutta method, and Finite difference method (FDM) [24, 25]. In this article, the fourth-order Runge-Kutta method (RK4) is applied to solve the model (1) because of its higher order of accuracy and unconditional stability. More information regarding fourth-order Runge-Kutta method can be found in Appendix 11. MATLAB R2020a is used as a programming language to implement the RK4 method for the system (1). Corresponding graphs of numerical simulation are presented in Section 5.2. Since the model (1) is a population model and monitors the dynamics of disease outbreaks in individuals, all the dependent variables and parameters must be non-negative. Fitting methodology like longitudinal daily case notification data or least-squares approach, Latin hypercube sampling can be imposed to execute a better fit for the model considering collected data and to estimate a set of parameters [27]. For the proposed model, the set of parameters like γ , β , α , l , and δ is estimated using the least-squares approach. The MATLAB GlobalSearch algorithm is examined to search for the best appropriate parameters from the Latin hypercube sampling. In Table 1, the best-estimated values of parameters regarding the model and data are presented, and we have used them to examine numerical simulation.

TABLE 1. Model parameters estimation.

Parameter	Value	Source
Λ	60	[28]
μ	0.002	[7]
γ	0.8975	Estimated
β	0.000011625	Estimated
δ	0.01	Estimated
l	0.005	Estimated
α	0.0000025	Estimated

5.2. Numerical Illustrations. Since November 2017, diphtheria outbreaks among the refugees have become a public health crisis with the initial index case reported on November 10th, 2017, in the Balukhali camp. This upper respiratory tract disease diphtheria is highly transmissible and is caused by the bacterium *Cyanobacteria diphtheria*, which escalates through air and water droplets and close physical contact. Bar diagram 2 (left) represents the

confirmed daily diphtheria cases in the Balukhali Rohingya camp for the first fifty days. Initially, for the first 20 days there were minimal cases of infection. However, within the next time-span of 5 days, the numbers crossed 50, and from day 25 to day 35, diphtheria cases increased significantly and peaked. Eventually, the number of infected populations gradually declined.

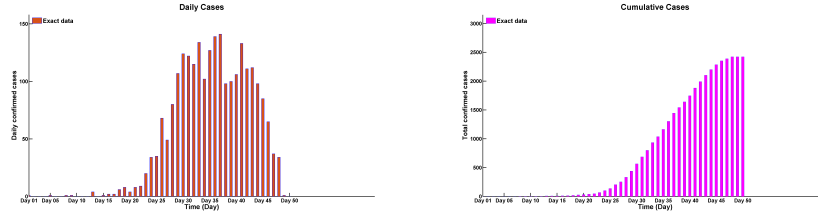


FIGURE 2. Bar diagram for (a) daily confirmed cases, and (b) cumulative data.

Figure 2 (right) portrays the total number of cases for fifty days. We see that within fifty days the total number of infected population cross 2000. Based on the current scenario, the assumption of the future forecast is discussed in the following figures.

In the deterministic model (1) we consider γ as the recovery rate for the infected population. Figures 3 and 4 show predicted results for different values of γ .

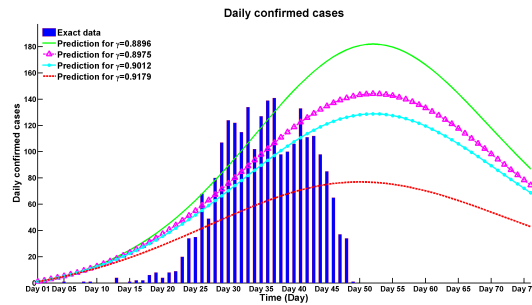


FIGURE 3. Effect of the parameter γ on the population of infected individuals per day.

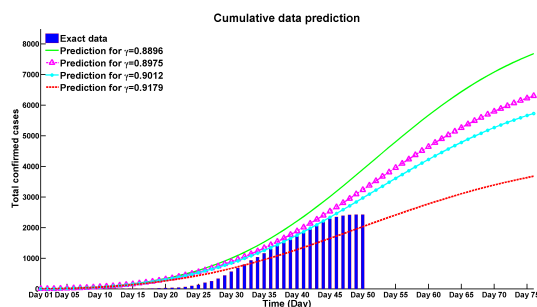


FIGURE 4. Effect of the parameter γ on the total number of infected individuals.

From Figure 3, the daily infected individual may increase for a certain time-span and it may last for ten to fifteen days. After that, the number of infected populations will decrease gradually, and eventually, there will be no infected population, consequently an increase in the recovery class can be noticed. High recovery rate results in lower cases of infection. We may predict the same outcome for the total number of infected cases from Figure 4. When the value of $\gamma = 0.9175$ ($R_0 = 0.378965$), the total number of infections can never cross 5000 and after a time long its value will be constant between 4000 to 5000. Whenever $\gamma = 0.8896$ ($R_0 = 0.390824$), the total number of infected population will be approximately 9000. To summarize, there will be an 80% change in infection rate as the value of γ by 3.14% is altered. Thus, the infection can be diminished if there is a rise in the recovery rate among the population.

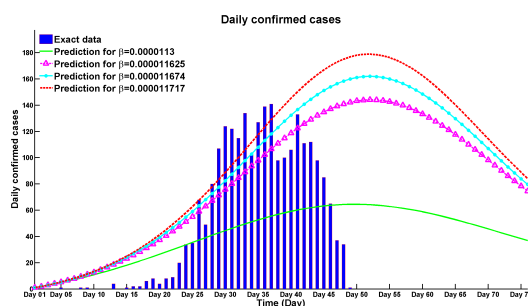


FIGURE 5. Effect of the parameter β on the population of infected individuals per day.

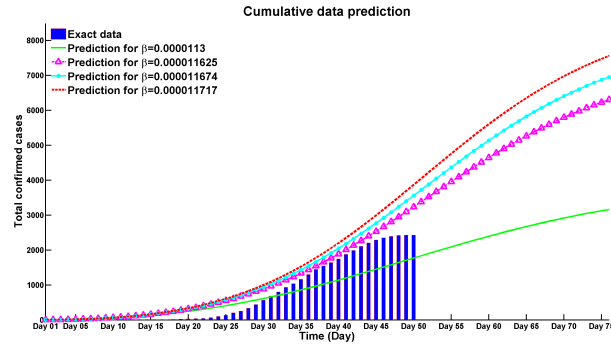


FIGURE 6. Effect of the parameter β on the total number of infected individuals.

In our formulated model, β is the infection transmission rate from susceptible individuals to infected populations. Figures 5 and 6 represent the future forecast of infected individuals for different values of β . From both of the figures, it is evident that a higher transmission rate implies a higher number of the infected population. For the value of $\beta = 0.000011717$ ($R_0 = 0.390457$), the solid red line presents the changes in population for both Figures 5 and 6. From Figure 5, it is evident that for $\beta = 0.000011717$ the maximum number of daily infected individuals may be around 180. Meanwhile, for $\beta = 0.0000113$ ($R_0 = 0.376561$) (the solid green line), the number of daily infected populations will not cross 80. Thus, the daily number of infected cases may change rapidly for very small changes of β , and this prediction is also true for cumulative data Figure 6.

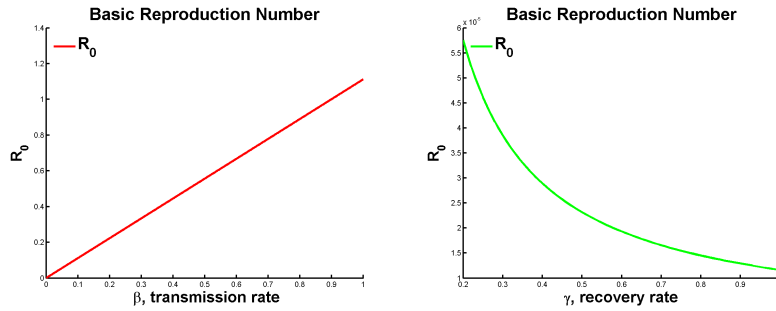


FIGURE 7. Estimated values of basic reproduction number with respect to β (left) and γ (right).

The basic reproduction number (R_0) is significant in decision-policy in an ongoing epidemic situation when exploring a model. Based on our postulated

model, we have illustrated how R_0 alters with different values of β and γ . Figure 7 (right) indicates that R_0 drops as the value of γ increases, where γ is the recovery rate of infected individuals. Increasing the pace of recovery across populations can thus be a powerful method for preventing diphtheria occurrences in Rohingya refugee camps. Diagram 7 (left) indicates that increasing the values of β enhances R_0 , where β is the transmission rate between susceptible and infected populations. As a result, in order to fend off diphtheria epidemics, we must minimize the infection transmission rate.

6. Conclusion

This article discusses a demographic SLIR epidemic model with numerical demonstrations. In this model, the Rohingya population is incorporated to study the transmission and recovery rates which depend on the diphtheria outbreak of 2017. In this study, we discuss the basic reproduction number and its impact on the disease outbreak for different values of parameters. To analyze a model, the basic reproduction number plays a vital role in decision-making in an ongoing outbreak situation. We have shown the changes in R_0 for different values of β and γ based on our assumed model. In diagram 7 (left), we see that by increasing the values of β the basic reproduction number is also increasing where β is the contact rate between susceptible population to infected individuals. Thus, to prevent diphtheria breakouts we must control the infection transmission rate which is a dominant sensitive parameter for understanding the transmission dynamics. On the other hand, Figure 7 (right) shows basic reproduction number decreases as the value of γ is increased where γ is the recovery rate of infected individuals. Thus, increasing the recovery rate among the populations can be a strong strategy to prevent diphtheria flare-outs in Rohingya refugee camps. The dynamical behavior of the model is discussed concerning distinct values of transmission and recovery rate. After analyzing the diagram, it is evident that diphtheria outbreaks can be controlled by taking some efficient actions. In the future, such analysis can help experimental workers and decision-makers to build a strong strategy to control the diphtheria outbreak rapidly in other regions. The sleazy living conditions like insufficient health care system, lack of proper drinking water, sanitation, and poor hygiene condition; infectious disease outbreaks are seen in refugee camps. This kind of ambient can increase the transmission of various infectious diseases such as cholera, hepatitis, diphtheria, and other transmitted diseases. Hence, it is necessary to consider climate changes and environmental variability while supplying clean water, and other essentials in the camp while increasing strong leadership internationally and sustainable investment. In this article, we do not consider any seasonal variability. People who are interested in working on this model can add this factor. Moreover, the model can be converted to a stochastic system to observe the discrepancy of the dynamics.

7. Acknowledgement

The authors' acknowledged to the anonymous reviewers for their suggestions which significantly improved the quality of the manuscript. The author MK acknowledged to the Bose Center for Advanced Study and Research in Natural Sciences for supporting research and students.

8. Ethical considerations

The Ethics Review Committee of Dhaka University approved the research protocol. No consent is required to publish this manuscript.

9. Funding

The research by M. Kamrujjaman was partially supported by the University Grants Commission, and Dhaka University Centennial Research Program, Bangladesh.

10. Conflict of interest

The authors declare no conflict of interest.

11. Appendix A

Runge-Kutta Method

Runge-Kutta (RK) method is one of the efficient finite difference schemes for first order ordinary differential equations with boundary conditions. Here, the fourth-order Runge-Kutta method is considered which is also known as "the classic Runge-Kutta method". Let us consider the first order initial-value problem.

$$(8) \quad \begin{cases} y' = F(x, y), & a \leq x \leq b, \\ y(a) = y_0. \end{cases}$$

The time step is given by, $\tau_i = \tau_0 + ih$ where h is the time step size. For the ODE (8), let $\omega_0 = a$ and for the next time step τ_{i+1} , the spatial component $y(\tau_{i+1})$ is given by

$$(9) \quad \omega_{i+1} = \omega_i + \frac{1}{6}(L_1 + 2L_2 + 2L_3 + L_4),$$

and

$$(10) \quad \begin{cases} L_1 = h * F(\tau_i, \omega_i), \\ L_2 = h * F(\tau_i + \frac{m}{2}, \omega_i + \frac{L_1}{2}), \\ L_3 = h * F(\tau_i + \frac{m}{2}, \omega_i + \frac{L_2}{2}), \\ L_4 = h * F(\tau_i + m, \omega_i + L_3). \end{cases}$$

Here, the method has four steps, where the former two are predictor steps and the latter are corrector steps. The Runge-Kutta method is a well-established method that is unconditionally stable with a total accumulated error of order $\mathcal{O}(h^4)$ and truncation error of order $\mathcal{O}(h^5)$ [29].

References

- [1] R. Matsuyama, A. R. Akhmetzhanov, A. Endo, H. Lee, T. Yamaguchi, S. Tsuzuki, and H. Nishiura, Uncertainty and sensitivity analysis of the basic reproduction number of diphtheria: a case study of a Rohingya refugee camp in Bangladesh, November–December 2017, *PeerJ*, 6:e4583, (2018).
- [2] W. O. Kermack, A. G. McKendrick, A contribution to mathematical theory of epidemics, *Proc. Roy. Soc. Lond. A.*, 700-721, (1927).
- [3] M. I. Simoya, J. P. Aparicio, Ross-Macdonald Models: Which one should we use? *Acta Tropica*, 105452, (2020).
- [4] A. Zeb, E. Alzahrani, V. S. Ertuk, G. Zaman, Mathematical model for coronavirus disease 2019 (COVID-19) containing isolation class, *Biomed Res Int.* Jun 25; 2020:3452402, (2020).
- [5] Z. Zhang, A. Zeb, E. Alzahrani, S. Iqbal, Crowding effects on the dynamics of COVID-19 mathematical model, *Adv Differ Equ*, 675, (2020).
- [6] Z. Zhang, R. Gul, A. Zeb, Global sensitivity analysis of COVID-19 mathematical model, *Alex. Eng. J.*, Volume 60, Issue 1, 565-572, (2021).
- [7] M. Hassan, M. Mahmud, K. Nipa, M. Kamrujjaman, Mathematical Modeling and COVID-19 Forecast in Texas, USA: A Prediction Model Analysis and the Probability of Disease Outbreak, *Disaster Medicine and Public Health Preparedness*, 1-27, (2021).
- [8] F. Finger, S. Funk, K. White, R. Siddiqui, W. J. Edmunds, and A. J. Kucharski, Real-time analysis of the diphtheria outbreak in forcibly displaced Myanmar nationals in Bangladesh, *BMC Med.*, (2018).
- [9] M. Paoluzzi, N. Gnan, F. Grassi, M. Salvetti, N. Vanacore, and A. Crisanti, A single-agent extension of the SIR model describes the impact of mobility restrictions on the COVID-19 epidemic, *Sci. Rep.*, 11:24467, (2021).
- [10] M. Torrea, J. L. Torrea, and D. Ortégaz, A modeling of a Diphtheria epidemic in the refugees camps, *bioRxiv*, (2017).
- [11] M. S. Mahmud, M. Kamrujjaman, & M. S. Islam, A spatially dependent vaccination model with therapeutic impact and non-linear incidence. *LNME*, 323e345, (2021).
- [12] M. Kamrujjaman, M. S. Mahmud, & M. S. Islam, Dynamics of a diffusive vaccination model with therapeutic impact and non-linear incidence in epidemiology. *J. Biol. Dyn.*, 15(sup1), S105eS133, (2020).
- [13] K. Sornbundit, W. Triampo, C. Modchang, Mathematical modeling of diphtheria transmission in Thailand, *Comput. Biol. Med.*, 87, 162–168, (2017).
- [14] A. Golaz, I. R. Hardy, P. Strebel, K. M. Biscard, C. Vitek, T. Popovic, and M. Wharton, Epidemic Diphtheria in the Newly Independent States of the Former Soviet Union: Implications for Diphtheria Control in the United States, *J. Infect. Dis.* 181(Suppl 1), S237–43, (2000).
- [15] M. R. Rahman, K. Islam, Massive diphtheria outbreak among Rohingya refugees: lessons learnt, *J. Travel Med.*, Volume 26, Issue 1, 2019.
- [16] J. A. Polonsky, M. Ivey, M. K. A. Mazhar, Z. Rahman, O. I. P. de Waroux, B. Karo, K. Jalava, S. Vong, A. Baidjoe, J. Diaz, F. Finger, Z. H. Habib, C. E. Halder, C. Haskew, L. Kaiser, A. S. Khan, L. Sangal, T. Shirin, Q. A. Zaki, M. A. Salam, K. White, Epidemiological, clinical, and public health response characteristics of a large outbreak of diphtheria among the Rohingya population in Cox’s Bazar, Bangladesh, 2017 to 2019: A retrospective study, *PLoS Med.*, 18(4), e1003587, (2021).

- [17] S. Ahmed, W. P. Simmons, R. Chowdhury, S. Huq. The sustainability–peace nexus in crisis contexts: how the Rohingya escaped the ethnic violence in Myanmar, but are trapped into environmental challenges in Bangladesh, Springer, 2021.
- [18] T. Waezizadeh, A. Mehrpooya, M. Rezaeizadeh, S. Yarahmadian, Mathematical models for the effects of hypertension and stress on kidney and their uncertainty, *Math. Biosci.*, Vol. 305, 77-95, (2018).
- [19] M. Kamrujjaman, M. S. Mahmud, & M. S. Islam, Coronavirus outbreak and the mathematical growth map of COVID-19. *Annual Research & Review in Biology*, 72e78, (2020).
- [20] M. Kamrujjaman, M. S. Mahmud, S. Ahmed, M. O. Qayum, M. M. Alam, M. N. Hassan, M. R. Islam, K. F. Nipa and U. Bulut. SARS-CoV-2 and Rohingya Refugee Camp, Bangladesh: Uncertainty and How the Government Took Over the Situation, *Biology*, 10, 124, 1-18, (2021).
- [21] M. A. Kuddus, and A. Rahman, Analysis of COVID-19 using a modified SLIR model with nonlinear incidence, *Results Phys.*, 27, 104478, (2021).
- [22] J. J. Tewa, R. Fokouop, B. Mewoli, and S. Bowong, Mathematical analysis of a general class of ordinary differential equations coming from within-hosts models of malaria with immune effectors, *Appl. Math. Comput.*, 218, 7347-7361, (2012).
- [23] M. Kamrujjaman, P. Saha, M. S. Islam, and U. Ghosh, Dynamics of SEIR Model: A case study of COVID-19 in Italy, *Results in Control and Optimization*, 7, 100119, (2022).
- [26] H. Nishiura, Correcting the Actual Reproduction Number: A Simple Method to Estimate R_0 from Early Epidemic Growth Data, *IJERPH*, 7(1), 291-302, (2010).
- [24] J. D. Murray, *Mathematical Biology I: An Introduction*, third edition, Springer, 2002.
- [25] M. Martcheva, *An Introduction to Mathematical Epidemiology*, Springer, 2015.
- [27] M. S. Mahmud, M. kamrujjaman, M. M. I. Y. Adan, M. A. Hossain, M. M. Rahman, M. S. Islam, M. Mohebujjaman, and M. M. Molla, Vaccine efficacy and SARS-CoV-2 control in California and U.S. during the session 2020-2026: A modeling study, *Infect. Dis. Model.*, 7: 62-81, (2021).
- [28] TIME. About 60 Rohingya Babies Are Born Every Day in Refugee Camps, the U.N. Says — TIME. 2018. Available online: <https://time.com/5280232/myanmar-bangladesh-rohingya-babies-births/> (accessed on 18 September (2020)).
- [29] R. L. Burden, R. L. Faires, *Numerical Analysis*. 9th Edition, Brookscole, Boston, 259-253, 2011.

ASMA AKTER AKHI
ORCID NUMBER: 0000-0002-4398-4287
DEPARTMENT OF MATHEMATICS
UNIVERSITY OF DHAKA
DHAKA 1000, BANGLADESH
Email address: akhiasma752@gmail.com

FARAH TASNIM
ORCID NUMBER: 0000-0003-3461-5647
DEPARTMENT OF MATHEMATICS
UNIVERSITY OF DHAKA
DHAKA 1000, BANGLADESH
Email address: ftnabila30@gmail.com

SAIMA AKTER
ORCID NUMBER: 0000-0001-9472-0524
DEPARTMENT OF MATHEMATICS
UNIVERSITY OF DHAKA
DHAKA 1000, BANGLADESH
Email address: aktersaima1995@gmail.com

MD. KAMRUJJAMAN
ORCID: 0000-0002-4892-745X
DEPARTMENT OF MATHEMATICS
UNIVERSITY OF DHAKA
DHAKA 1000, BANGLADESH
Email address: kamrujjaman@du.ac.bd